



# “Ballistic” waves among chemically oscillating micromotors†

 Qizhang Wang,‡ Chao Zhou,‡ Luyang Huang and Wei Wang \*

 Cite this: *Chem. Commun.*, 2021, 57, 8492

 Received 15th May 2021,  
Accepted 25th July 2021

DOI: 10.1039/d1cc02558a

[rsc.li/chemcomm](http://rsc.li/chemcomm)

**Coordinating a group of chemically powered micromotors holds great importance in potential applications that involve a large population in a complex environment, yet information transmission at a population scale remains challenging. To this end, we demonstrate how propagating waves emerge among a population of spontaneously oscillating micromotors that dash toward a direction prescribed by their Janus orientations (termed a “ballistic” wave). Moreover, chemical communication among these micromotors enables the tuning of the speed and frequency of individual micromotors and their waves, by varying the population density or the viscosity of the medium.**

The research of chemically powered, autonomously moving micromotors has received mounting interest in recent years,<sup>1–4</sup> fueled by the popular imagination of nanorobots capable of biomedical and environmental applications.<sup>5–7</sup> The successful operation of these micromotors, however, often requires long-range information transmission and coordination among a large population. For chemical micromotors, the most straightforward way to achieve such communication is by the transport of chemical signals.<sup>8</sup> However, they diffuse slowly and decay over space and time, posing a serious limit to the long-range chemical communication among chemical micromotors.<sup>9–13</sup>

The recent discovery of silver (Ag)-containing oscillating micromotors, by the Sen lab in the early 2010s,<sup>14</sup> ushers in a new, biomimetic strategy for chemically communicating micromotors. In a series of reports, AgCl or Ag<sub>3</sub>PO<sub>4</sub> microparticles were found to alternate between fast and slow periods of motion, and even give rise to propagating waves at higher population densities.<sup>14</sup> Across the wavefronts, particles alternate either between aggregation and dispersion,<sup>15</sup> or between stick and slip motion,<sup>14</sup> but their kinetics were difficult to identify. Inspired by these early studies, we have recently

investigated the mechanisms of the individual oscillation of Ag-coated Janus microspheres,<sup>16</sup> how their dynamics are sensitive to switching light on and off,<sup>17</sup> how oscillating micromotors synchronize into collective beating,<sup>18</sup> and how they could “teach” other types of micromotors to oscillate.<sup>10</sup> However, little remains known on the dynamics of waves emerging from these oscillating motors, or how a wave can be tuned. Filling this gap holds practical values for designing a wave-based communication strategy among a large population of chemical micromotors.

In this communication, we show experimentally that a Janus micromotor half-coated with Ag form traveling waves, where each motor on the wavefront moves “ballistically” in a direction dictated by its Janus interface (referred to as a “ballistic wave”). Moreover, the peak speeds and frequency of either an individual micromotor or a wave can be continuously tuned by altering the population density or the viscosity of the medium. This study suggests that oscillating micromotors could be useful for complex tasks that require spontaneous coordination.

We begin with a very brief introduction to the operating principles of Ag-containing, oscillating micromotors. In our experiments, they typically take the form of an inert microsphere (*e.g.* polymethyl methacrylate, or PMMA) half coated with Ag *via* physical vapor deposition (see Fig. S1, ESI† for characterizations). When immersed in an aqueous solution of H<sub>2</sub>O<sub>2</sub>, KCl, and irradiated with UV light, these Ag Janus spheres alternate between an episode of fast, autonomous motion directed away from the Ag cap, and a slow, diffusive episode that lasts for a few seconds<sup>16</sup> (Fig. 1a and see Video S1, ESI† for a typical example). It has been hypothesized that such an oscillation dynamic originates from a chemical oscillation between Ag and its oxidized form AgCl on the surface of a Ag-coated microsphere.<sup>16</sup> This pair of reactions then produce time-varying chemical gradients of ions that give rise to ionic self-diffusiophoresis,<sup>19–22</sup> an electrokinetic mechanism that propels the microsphere into intermittent motion. However, the exact pathway of this chemical oscillation, and the identity of the chemical species released, remain unknown at this point.

School of Materials Science and Engineering, Harbin Institute of Technology (Shenzhen), Shenzhen, Guangdong 518055, China. E-mail: weiwangsz@hit.edu.cn

† Electronic supplementary information (ESI) available. See DOI: 10.1039/d1cc02558a

‡ These two authors contributed equally.

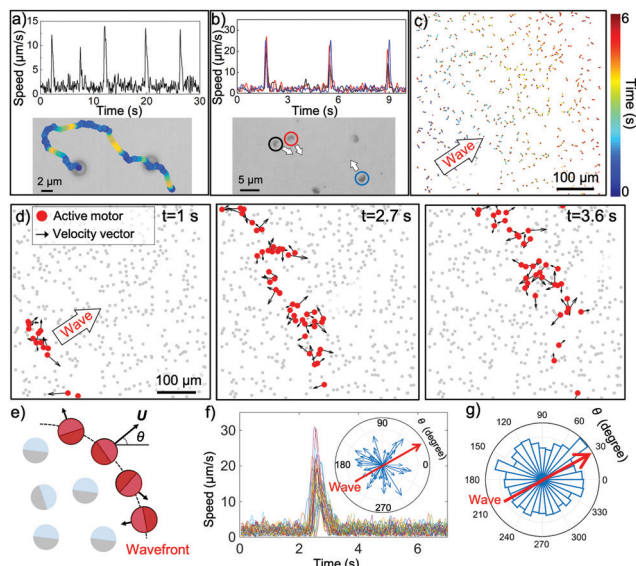


**Fig. 1** Oscillating micromotors and their ballistic waves. (a) Dynamics of single oscillating micromotor. top panel: instantaneous speed profile of one PMMA-Ag oscillating micromotor; bottom panel: its trajectory color-coded with its instantaneous speeds; (b) Three synchronized, adjacent oscillating micromotors. top panel: instantaneous speed profiles; bottom panel: moving directions (white arrows) of the three micromotors; (c) A representative ballistic wave propagating from the lower left to the top right corner among a population of oscillating micromotors, with trajectories of all motors color-coded with time. The ones that move at the earliest time are labelled blue. (d) Wavefronts of the ballistic wave in (c) visualized by marking the activated micromotors as red dots and their instantaneous velocities (both the direction and the magnitude) in black arrows; (e) Scheme of active particles located at wavefront. (f) Instantaneous speed profiles of all micromotors activated at  $t = 2.7$  s in (d) over time as the wave passes (insert: their velocity vectors at  $t = 2.7$  s, showing how activated motors at a wavefront in fact move ballistically in all directions); (g) distribution of the directionality of a total of 230 active particles located at all wavefronts in the entire Video S2 (ESI<sup>†</sup>).

One of the most remarkable features of these oscillating micromotors is the emergence of collective behaviors.<sup>14,15,18,23</sup> We have shown earlier that as they get closer, the chemicals released by one motor affects the chemical kinetics of the other, pushing and pulling on each other's chemical clock. Quite abruptly, their oscillation synchronizes (Fig. 1b), and a cluster of Ag Janus micromotors beats in unison.<sup>18</sup> However, when examining the entire field of view populated with many separate particles, such as that shown in Fig. 1c, we see that such synchronization does not mean every motor is activated simultaneously everywhere in the population (like in the case of fireflies),<sup>24</sup> but rather with a slight phase lag across the field of view, thus taking the form of a traveling wave (see Video S2, ESI<sup>†</sup>) in a way reminiscent of phase waves found in many natural systems,<sup>25,26</sup> or the so-called Mexican waves in a football stadium.<sup>27</sup> We note that although these microparticles are uniformly illuminated, waves originate at seemingly random spots and propagate outwards.

One of the key findings reported here is that micromotors on the same wavefront are activated synchronously in time, but move in random directions. This is referred to as a “ballistic

wave”. A typical example is given in Video S2 (ESI<sup>†</sup>) and Fig. 1d, where PMMA-Ag Janus microspheres of 2.5  $\mu\text{m}$  in diameter and a population density (packing fraction) of  $\sim 1.3\%$  were mixed with aqueous solutions of  $\text{H}_2\text{O}_2$  of 0.5 wt% and KCl of 400  $\mu\text{mol L}^{-1}$ , and illuminated uniformly with a mercury lamp of 230  $\text{mW cm}^{-2}$ . A wave begins with a narrow band of micromotors moving ballistically from the bottom left corner of the field of view, followed by their neighbours located to their top right, and so on. As a result, a wave of action propagates through the entire population from the bottom left to the top right (Fig. 1c).

To examine the individual dynamics of a micromotor on a wavefront, a more zoomed-in view of a wave is presented in Fig. 1d, where micromotors above a threshold speed (e.g., 5  $\mu\text{m s}^{-1}$ ) are highlighted as red dots, and their instantaneous velocities are shown in black arrows that point in seemingly random directions. This dynamic of simultaneous activation but random direction is further quantified in Fig. 1e–g, which show that the speed profiles of 40 micromotors along the same wavefront overlap with each other in time (Fig. 1f), yet their velocity vectors point in completely different directions with similar probabilities (Fig. 1f, inset), uncorrelated with the wave direction (red arrow). A survey of the moving direction of all active micromotors (a total of 230) on every wavefront in Video S2 (ESI<sup>†</sup>) is compiled in Fig. 1g, further suggesting that oscillating micromotors in a ballistic wave are *temporally but not spatially synchronized*.

We propose that a ballistic wave is the response of many individual micromotors to a propagating chemical wave. There are two pieces of evidence. First, an “activated” micromotor at a wave front moves in the direction vertical to its Janus interface and away from the Ag coated cap (Fig. S3 and Video S3, ESI<sup>†</sup>), which is the natural direction of an oscillating micromotor during its activated pulses. Second, we mixed “active” PMMA-Ag motors with polystyrene microspheres that served as inert tracers (Fig. 2 and Video S4, ESI<sup>†</sup>), and saw that only those containing Ag were activated by an incoming wave and pulsed, while chemically inert tracer spheres remained mostly Brownian. The most likely mechanism responsible for these two observations is that an incoming chemical signal that propagates as waves triggers the chemical reaction on a Janus microsphere, so that it undergoes a chemical oscillation that leads to fast motion. The possible roles of hydrodynamics and electrokinetics (electro-phoresis and -osmosis) are subject to further studies.

A ballistic wave described above is fundamentally different from waves reported earlier either with Ag-containing microparticles,<sup>14,15,23</sup> or those found in classic systems of oscillating entities such as Belousov–Zhabotinsky (BZ) reactions or living organisms.<sup>28–34</sup> In the former case, the oscillation of  $\text{Ag}_3\text{PO}_4$  or  $\text{AgCl}$  particles gives rise to travelling waves in which each particle alternates either between aggregation and dispersion,<sup>15</sup> or between stick and slip motion.<sup>14</sup> In contrast, in the current experiment Janus motors on the wavefronts clearly showed autonomous, directional motion when activated. In the latter case, although chemical waves are commonly found in

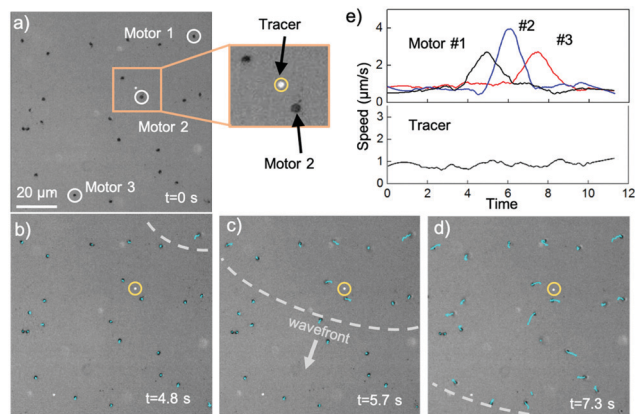


**Fig. 2** Active and inert microspheres in a ballistic wave. (a–d) Time-stamped optical micrographs of the propagation of a wave across a population of PMMA-Ag micromotors (black dots) mixed with a small amount of fluorescent polystyrene tracer microspheres (appear white). One of such tracer spheres is highlighted with a yellow circle in the inset. (e) Speeds of three active motors circled in white in (a) sequentially rose and fell over time as a wave passed, while the speeds of the tracer particle remained small and fluctuating.

many natural or synthetic systems across a wide range of scales, rarely does one see microscopic objects moving in response to the waves, not to mention in a way that is correlated with its self-propulsion (*i.e.*, “ballistic”). Although different in the way waves are manifested, both the BZ systems and the ballistic waves reported here are a result of chemical communications among chemically active entities in a solution.

The nature of chemical communication in a ballistic wave of oscillating micromotors also offers the possibility to tune how each motor is coupled to each other, and thus the dynamics of the resulting wave. This can be done by varying how close micromotors are (*via* the population density), or by tuning how fast the chemical signal diffuses (*via* the medium viscosity). We first examine how population density affects the dynamics of oscillating motors, both for individuals and for ballistic waves. Typical results are given in Fig. 3 and Video S5 (ESI<sup>†</sup>). When compared side by side in Fig. 3a, it is clear that three uncorrelated, oscillating motors at a low particle density  $\phi$  (left,  $\phi = 0.4\%$ ) pulsates with larger peak speeds but smaller frequencies than their counterparts in a more concentrated suspension (right,  $\phi = 1.5\%$ ). More quantitatively, we see in Fig. 3b that, as the population density  $\phi$  increases, the peak speeds of oscillating motors (hollow red data) monotonically decrease, yet their pulsing frequencies (solid black data) show an opposite trend. In other words, motors pulse less strongly but more frequently when they see more neighbours, which strongly suggests that the chemical coupling between each motor not only affects the phases of their oscillations (therefore causing synchronization),<sup>18</sup> but also their chemical kinetics (*i.e.* speeds and frequencies). The underlying mechanism is possibly related to the amount of Ag, or the local H<sub>2</sub>O<sub>2</sub> concentration, *etc.*, but the details of how this arises remain unknown at this point.

In the case of wave dynamics (Fig. 3c), increasing the particle density causes each activated motor at a wavefront to pulse less strongly (red circle data), similar to how individual micromotors

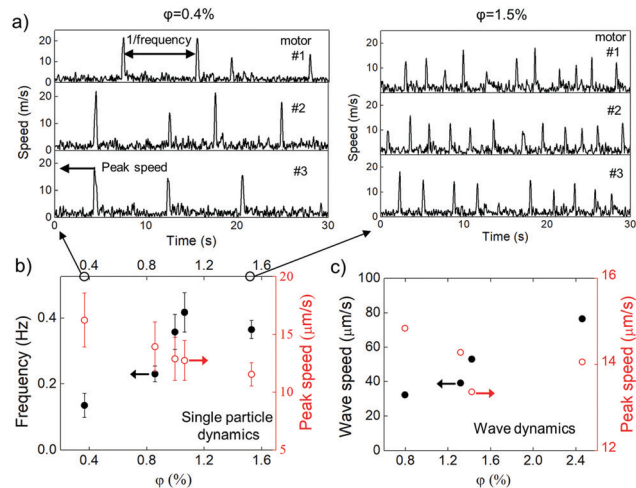


**Fig. 3** Dynamics of individual oscillating micromotors and their ballistic waves at different particle densities  $\phi$ . (a) Instantaneous speed profiles of three representative micromotors at low ( $\phi = 0.4\%$ ) and high ( $\phi = 1.5\%$ ) particle density; (b) Oscillating frequencies and peak speeds of individual motors at various particle densities; (c) Wave speeds and the peak speeds of motors at water fronts at different particle densities.

behave in Fig. 3b (but to a lesser degree). Moreover, waves sweep faster across a denser population (black solid data), likely because it now takes less time for the chemical signal to diffuse and reach the next motor.

A second way to tune the inter-motor coupling is to vary the medium viscosity  $\eta$ , by adding different amount of glycol in an aqueous suspension of motors (see Table S1, ESI<sup>†</sup> for viscosity measurement). Results are shown in Fig. 4 and Video S6 (ESI<sup>†</sup>). The medium viscosity affects the speed of an electrokinetically propelled micromotor  $U$ , *via* (assuming permittivity  $\epsilon$  unchanged)  $U = \epsilon\zeta E/\eta$ , where  $\epsilon$  is the electrical permittivity of the medium,  $\zeta$  is the zeta potential of the motor surface, and  $E$  is the electric field arising from the asymmetric diffusion of the chemical species (assumed to be Ag<sup>+</sup> and Cl<sup>-</sup> in this case,<sup>16,35</sup> and assumed to be a constant). As a result, single motors slow down in a more viscous solution, with a speed that scales (roughly) linearly with  $1/\eta$  (Fig. 4a). We note that the magnitude of  $E$  could also be dependent on  $\eta$ , because  $\eta$  affects both the diffusivity of ions and possibly reaction kinetics. The detail of how  $E$  is connected to  $\eta$  is subject to further studies.

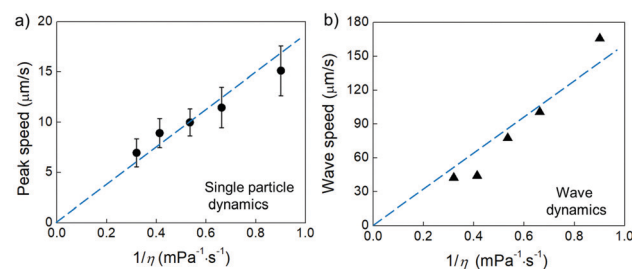


**Fig. 4** Speeds of individual oscillating micromotors (a) and their ballistic waves (b) in solutions of different viscosities  $\eta$ . Dashed lines are linear fits through the origin.



In addition, medium viscosity also modulates how fast a chemical signal diffuses between two motors *via*  $D = kT/6\pi\eta a$ , where  $D$  and  $a$  are the diffusion coefficient and the radius of the chemical signal species, respectively, and  $kT$  is the thermal energy. Fig. 4b shows a linear scaling between the wave speeds and the inverse of the medium viscosity, similar to how viscosity affects individual micromotors, suggesting that information transmission slows down as the medium viscosity increases.

In conclusion, we report the discovery of “ballistic waves” among oscillating, Ag-containing micromotors, where motors on the wavefronts move synchronously in time, but in directions dictated by their own Janus interfaces. Moreover, because the inter-motor coupling relies on chemical communication, the dynamics of oscillating motors and their waves can be tuned *via* population density and medium viscosity. At higher population densities, oscillating micromotors move in shorter and weaker pulses, and ballistic waves travel faster, with each motor on the wavefront pulsating more weakly. Increasing the medium viscosity, on the other hand, consistently slows down both individual motors and their waves, likely because both a colloidal particle and a solute species diffuse more slowly in a more viscous medium.

Overall, this study reports a kind of “ballistic” waves consisting of sequentially activated Janus micromotors, which, to the best of our knowledge, is never demonstrated before. This observation suggests that the propagation of a chemical signal could trigger the motion of micromotors, providing the possibility for micromotors to achieve certain tasks *via* spontaneous coordination without external control. In particular, the fact that motor and wave dynamics are tuneable sheds light on understanding chemical communications and coordination between oscillating micromotors, and is also useful for designing and controlling their collective behaviours.

This project is financially supported by the Natural Science Foundation of Guangdong Province (No. 2017B030306005), National Natural Science Foundation of China (11774075), and the Science Technology and Innovation Program of Shenzhen (JCYJ20190806144807401). We are grateful for the helpful discussions with Profs. Hepeng Zhang, Darrell Velegol and Ayusman Sen.

## Conflicts of interest

There are no conflicts to declare.

## References

- 1 E. Karshalev, B. Esteban-Fernández de Ávila and J. Wang, *J. Am. Chem. Soc.*, 2018, **140**, 3810–3820.
- 2 B. Robertson, M.-J. Huang, J.-X. Chen and R. Kapral, *Acc. Chem. Res.*, 2018, **51**, 2355–2364.
- 3 S. Sánchez, L. Soler and J. Katuri, *Angew. Chem., Int. Ed.*, 2015, **54**, 1414–1444.
- 4 K. K. Dey, F. Wong, A. Altemose and A. Sen, *Curr. Opin. Colloid Interface Sci.*, 2016, **21**, 4–13.
- 5 J. G. S. Moo and M. Pumera, *Chem. – Eur. J.*, 2015, **21**, 58–72.
- 6 J. Li, B. Esteban-Fernández de Ávila, W. Gao, L. Zhang and J. Wang, *Sci. Rob.*, 2017, **2**, eaam6431.
- 7 W. Wang and C. Zhou, *Adv. Healthcare Mater.*, 2021, **10**, 2001236.
- 8 L. Huang, J. L. Moran and W. Wang, *JCIS Open*, 2021, 100006.
- 9 C. Chen, X. Chang, H. Teymourian, D. E. Ramírez-Herrera, B. Esteban-Fernández de Ávila, X. Lu, J. Li, S. He, C. Fang, Y. Liang, F. Mou, J. Guan and J. Wang, *Angew. Chem., Int. Ed.*, 2018, **57**, 241–245.
- 10 C. Zhou, Q. Wang, X. Lv and W. Wang, *Chem. Commun.*, 2020, **56**, 6499–6502.
- 11 F. Mou, X. Li, Q. Xie, J. Zhang, K. Xiong, L. Xu and J. Guan, *ACS Nano*, 2020, **14**, 406–414.
- 12 C. H. Meredith, P. G. Moerman, J. Groenewold, Y.-J. Chiu, W. K. Kegel, A. van Blaaderen and L. D. Zarzar, *Nat. Chem.*, 2020, **12**, 1136–1142.
- 13 C. Wu, J. Dai, X. Li, L. Gao, J. Wang, J. Liu, J. Zheng, X. Zhan, J. Chen, X. Cheng, M. Yang and J. Tang, *Nat. Nanotechnol.*, 2021, **16**, 288–295.
- 14 M. E. Ibele, P. E. Lammert, V. H. Crespi and A. Sen, *ACS Nano*, 2010, **4**, 4845–4851.
- 15 A. Altemose, M. A. Sánchez-Farrán, W. Duan, S. Schulz, A. Borhan, V. H. Crespi and A. Sen, *Angew. Chem., Int. Ed.*, 2017, **56**, 7817–7821.
- 16 C. Zhou, X. Chen, Z. Han and W. Wang, *ACS Nano*, 2019, **13**, 4064–4072.
- 17 X. Chen, C. Zhou, Y. Peng, Q. Wang and W. Wang, *ACS Appl. Mater. Interfaces*, 2020, **12**, 11843–11851.
- 18 C. Zhou, N. J. Suematsu, Y. Peng, Q. Wang, X. Chen, Y. Gao and W. Wang, *ACS Nano*, 2020, **14**, 5360–5370.
- 19 J. L. Moran and J. D. Posner, *Annu. Rev. Fluid Mech.*, 2017, **49**, 511–540.
- 20 X. Chen, C. Zhou and W. Wang, *Chem. – Asian J.*, 2019, **14**, 2388–2405.
- 21 D. Velegol, A. Garg, R. Guha, A. Kar and M. Kumar, *Soft Matter*, 2016, **12**, 4686–4703.
- 22 J. L. Anderson, *Annu. Rev. Fluid Mech.*, 1989, **21**, 61–99.
- 23 A. Altemose, A. J. Harris and A. Sen, *ChemSystemsChem*, 2020, **2**, e1900061.
- 24 S. Strogatz, *How Order Emerges from Chaos in the Universe, Nature, and Daily Life, Sync*, Hachette UK, 2012.
- 25 A. T. Winfree, *Faraday Symp. Chem. Soc.*, 1974, **9**, 38–46.
- 26 S. P. Parsons and J. D. Huizinga, *J. Physiol.*, 2018, **596**, 4819–4829.
- 27 I. Farkas, D. Helbing and T. Vicsek, *Nature*, 2002, **419**, 131–132.
- 28 P. M. Wood and J. Ross, *J. Chem. Phys.*, 1985, **82**, 1924–1936.
- 29 R. Kapral and K. Showalter, *Chemical Waves and Patterns*, Springer Science & Business Media, 2012.
- 30 H. Kitahata, N. Yoshinaga, K. H. Nagai and Y. Sumino, *Chem. Lett.*, 2012, **41**, 1052–1054.
- 31 J. E. Speksnijder, C. Sardet and L. F. Jaffe, *Dev. Biol.*, 1990, **142**, 246–249.
- 32 S. C. Müller, T. Mair and O. Steinbock, *Biophys. Chem.*, 1998, **72**, 37–47.
- 33 J. B. Chang and J. E. Ferrell Jr, *Nature*, 2013, **500**, 603–607.
- 34 R. Kapral, *Science*, 1985, **229**, 852–854.
- 35 C. Zhou, H. P. Zhang, J. Tang and W. Wang, *Langmuir*, 2018, **34**, 3289–3295.